Translation-rotation decoupling of colloidal clusters of various symmetries

Stephen M. Anthony,[1] Minsu Kim,[2] and Steve Granick[1,2,3,a)]
[1]*Department of Chemistry, University of Illinois, Urbana, Illinois 61801, USA*
[2]*Department of Physics, University of Illinois, Urbana, Illinois 61801, USA*
[3]*Department of Materials Science and Engineering, University of Illinois, Urbana, Illinois 61801, USA*

(Received 16 August 2008; accepted 18 November 2008; published online 22 December 2008)

Single-particle tracking was used to measure the diffusion in aqueous suspension of dilute colloidal clusters, 2–9 μm in size, fabricated by joining 1.57 μm spheres into planar arrangements of various particle numbers and symmetries (doublet, trimer, square, pentamer, hexamer, and so forth). They were allowed to sediment close to a glass surface and their Brownian motion parallel to the surface, effectively in a two dimensional (2D) geometry, was imaged in a microscope in the presence of 3 mM monovalent salt to essentially screen electrostatic interactions. Geometric asymmetry produced systematically increasing discrepancy between the equivalent hydrodynamic radius of translation and rotation—tabulated in this paper. Our observations include cases where the effective hydrodynamic radius changes more rapidly for translation than rotation, the converse, and also cases where the effective hydrodynamic radius for translation changes significantly, while that of rotation is effectively constant. The significance is to document the connection between translational and rotational 2D mobilities for geometrical shapes not described by the Stokes–Einstein–Debye equations for spherical particles. © *2008 American Institute of Physics*. [DOI: 10.1063/1.3043443]

I. INTRODUCTION

This paper, which capitalizes on recently developed imaging techniques in video microscopy, concerns direct observation of the Brownian motion of colloidal-sized particles at the single-particle level. Such particles are interesting due to their ubiquity in nature and technology and also their capacity to be imaged in a microscope while retaining key features of particles that are even smaller. On the technological side, colloids have found applications ranging from common materials such as paints and ceramics to advanced materials such as photonic crystals[1] and chemical sensors.[2] On the academic side, their capacity to be imaged has led to their employment as model systems in which to study generic physical problems such as crystal growth and structure,[3] the dynamics of glassy states,[4] and grain boundary formation in crystals.[5] In recent years, study has branched out from analysis of uniform spherical particles to colloids with more complicated geometry, including rods, disks, ellipsoids, and chemically heterogeneous particles.[6–8] The significantly more complex hydrodynamic interactions of such systems lead one, on physical grounds, to expect large differences when comparing these systems to more conventional ones based on uniform spheres. To understand this would be pertinent to understanding flow, gelation, and jamming of these materials. However, to date, fabrication has been primarily limited to structures of high symmetry (rod or disklike), thus missing the wealth of shapes present in nature.

Here we report the translational and rotational dynamics of a family of particles based on silica spheres welded together into planar clusters, with significant variation both in the number of spheres employed and the overall symmetry of the clusters. Taking this approach, we examine systematically the relative influence of cluster size and configuration upon the translational and rotational mobilities of colloidal particles when they undergo effectively two dimensional (2D) diffusion.

The significance is to document the connection between translational and rotational mobilities for geometrical shapes not described by the Stokes–Einstein–Debye equations for spherical particles. It is common practice to regard nonspherical particles in terms of their equivalent hydrodynamic radius, the size of a sphere that would display similar dynamical behavior. Here, we show that cluster asymmetry causes systematic differences between the equivalent hydrodynamic radius for rotation and translation. Therefore, while translational diffusion is frequently a more accessible value than rotational diffusion, without knowing and understanding the geometry of a particle, it is not possible to determine the rotational diffusion from the translational diffusion.

II. EXPERIMENTAL SECTION

A. Samples

The clusters were fabricated by spreading a droplet of aqueous solution of 1.57 μm diameter colloidal silica particles (0.5% solid, Duke Scientific 8150) onto a microscope slide treated with piranha solution. Subsequent evaporation left a dispersed submonolayer of particles, with randomly distributed clusters ranging in typical size from two to nine colloids. During evaporation, the slide was manually tilted in such a fashion that the contact line moved across slide to avoid the "coffee ring" effect.[9] Electron beam deposition of a thin (30 nm) layer of SiO_2 bonded the spheres together.[8] The

a)Electronic mail: sgranick@uiuc.edu.

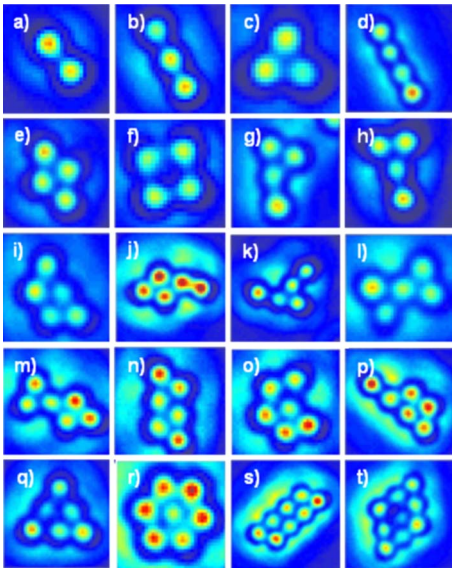

FIG. 1. (Color online) Examples of the microscopic shapes whose diffusion was studied; these images were taken *in situ* using differential interference contrast microscopy as described in the text. The elementary particle diameter is the same in each image, 1.57 μm, and the scale varies between images.

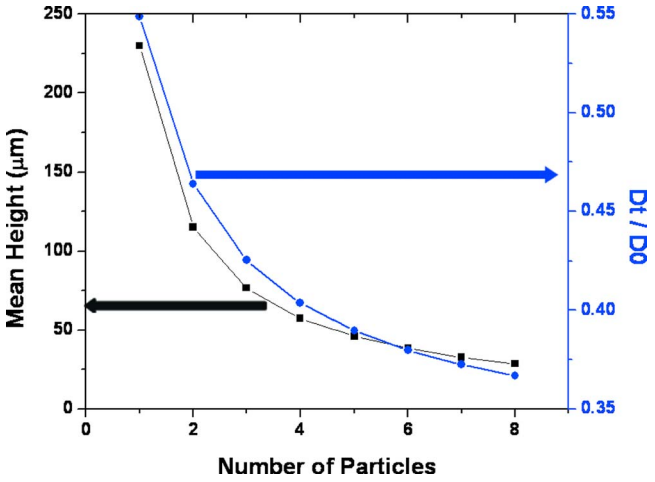

FIG. 2. (Color online) Left ordinate: the gravitational scale height computed from the Boltzmann distribution giving the average distance from the bottom wall vs the number of particles in the cluster. As the number of elemental particles and hence mass of the cluster increases, the expected mean separation of the bottom of the cluster from the wall decreases (squares). Right ordinate: the computed ratio between near-surface translational diffusion and translational diffusion in the bulk, for spheres described by Eq. (5) (circles).

large variety of structures generated using this fabrication method were planar; their microscopic images are shown in Fig. 1. A key point is that as the bonding layer of SiO_2 had the same chemical makeup as the parent silica particles, the resulting clusters were essentially homogeneous chemically.

The clusters were dispersed in a 3 mM KNO_3 aqueous solution such that the Debye length was screened to be negligible (5 nm) relative to the cluster size. Due to their density mismatch (1 g cm^{-3}), the clusters sedimented toward the bottom microscope slide, resulting in a Boltzmann distribution of elevation from the bottom. The gravitational scale height, which to a first approximation gives the average distance between the cluster and the bottom wall, was computed for each cluster and is plotted in Fig. 2 (together with the anticipated wall effect on translational diffusion, discussed below). The effects of entropic depletion of the clusters from the bottom wall, for all geometries other than the sphere, were not included in this or the following equations, however. Gravitational settling confined these structures to the image plane of the microscope. Further, gravitational settling against the bottom wall also limited the orientation of the clusters and confined the translation and rotation of the clusters to quasi-2D. Trivially, the cluster exhibiting the greatest deviation from 2D is cluster a, as it contains only two particles and experiences the least gravitational settling. Mathematically, for these purposes this cluster can be equivalently treated as an infinitely thin rod with length equal to the particle diameter, and the same mass as the cluster. The angles that the rod can sample are therefore limited based on the height of the center of the rod from the wall,

$$\theta \leq \arcsin\left(\frac{y}{r}\right), \tag{1}$$

where θ is the angle of the cluster with respect to the 2D plane, y is the height of the center of the rod from the wall, and r is the radius of the particle. Integrating the possible states with the probability distribution of heights above the wall, the probability that the angle which the axis of the cluster forms with the 2D plane is greater than θ and is given by

$$P(\theta) = e^{-r\sin(\theta)/h} - \sin(\theta)e^{-r/h} - \frac{r\sin(\theta)}{h}\int_{r\sin(\theta)}^{r}\frac{e^{-y/h}}{y}dy, \tag{2}$$

where h is the gravitational scale height. As can be seen in Fig. 3, the cluster deviates from 2D by more than 25° less

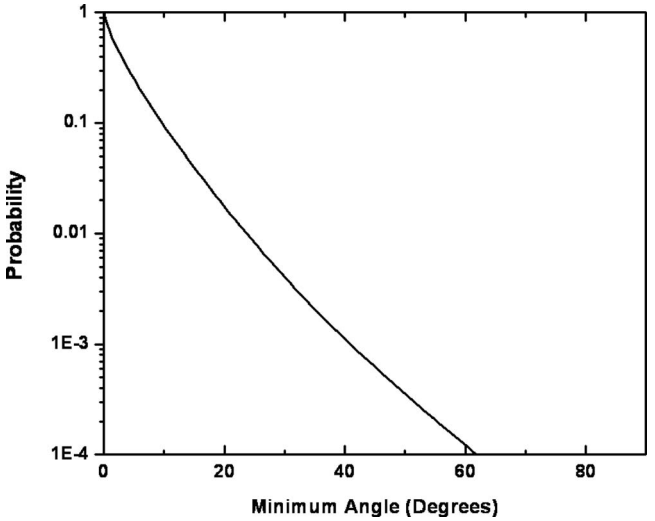

FIG. 3. Probability of deviation from the planar configuration was considered for the lightest anisotropic cluster, a two-sphere dumbell, in order to inspect the extent to which the systems studied in this paper can be considered as quasi-2D. The plot shows the fractional time that the axis of the dumbell deviates from the 2D plane by at least the angle specified in the abscissa. For this worst-case cluster, the deviation exceeds 25° less than 1% of the time.

than 1% of the time. Therefore, 99% of the time, the component of the cluster parallel to the 2D imaging plane is at least 95% of the value it would have if it were truly 2D. Therefore, even for the least 2D case we observe, quasi-2D analysis is appropriate, although undoubtedly this is partially responsible for the comparatively larger error bars for our measurements of diffusion for the clusters of two and three particles.

B. Microscopy

The mobility of the clusters was observed with white light illumination in a Zeiss Axiovert 200 inverted microscope configured in differential interference contrast mode. A 63× objective was employed, followed by 1.6× postmagnification. Time-sequence movies of translational and angular positions were recorded using a back-illuminated electron-multiplying charge coupled device camera (Andor iXON DV 897-BV), with an exposure time of 60 ms/frame. The intercluster separation was kept large, large enough that the influence of neighboring clusters was negligible.

Trajectories were analyzed using image analysis software developed in this laboratory and described elsewhere.[10] Translation and rotation about the center of mass of each cluster were computed from inspecting the trajectories of its spherical elements.

III. RESULTS AND DISCUSSION

A. Examples of raw data

The raw data consisted essentially of mean-squared displacements, both angular displacement around the center of mass of the cluster and translational displacement of the center of mass of the cluster. Regardless of cluster size and shape, both of these invariably gave trajectory characteristic of simple Fickian diffusion, as illustrated in Fig. 4(a). From this, the translational diffusion coefficient was readily computed using the following relation appropriate for diffusion in a plane:

$$\mathrm{MSD}_t(\Delta t) = 4D_t\Delta t. \tag{3}$$

Here, MSD_t is the translational mean-squared displacement of the center of mass, D_t is the translational diffusion coefficient, and Δt is the time elapsed. Similarly, by compensating for the looped nature of angle (θ) by allowing the angle to vary freely (values <0 or $>360°$), rotation about the center of mass follows the equivalent relation

$$\mathrm{MSD}_\theta(\Delta t) = 2D_\theta\Delta t, \tag{4}$$

where MSD_θ is the rotational mean-squared displacement of the center of mass, D_θ is the rotational diffusion coefficient, Δt is the time elapsed, and the constant of proportionality is reduced to 2 since just a single degree of freedom comes into play. We now make a parenthetical technical comment. The application of Eq. (4) is limited to the special case where the rotation is 2D or quasi-2D as we have here; for the case of three dimensional diffusion, the angle θ cannot be considered independently of the angle φ.

Examination of the displacement probability distribution revealed that both translational and rotational displacements were Gaussian, as should be the case for Brownian motion, as illustrated in Figs. 4(b) and 4(c). It is true that ellipsoidal particles were recently shown to display deviations from this relation.[6] Discrepancies of that kind were not observed here, partly because the aspect ratio of the present particles was smaller and partly because the present distributions were averaged over all orientations.

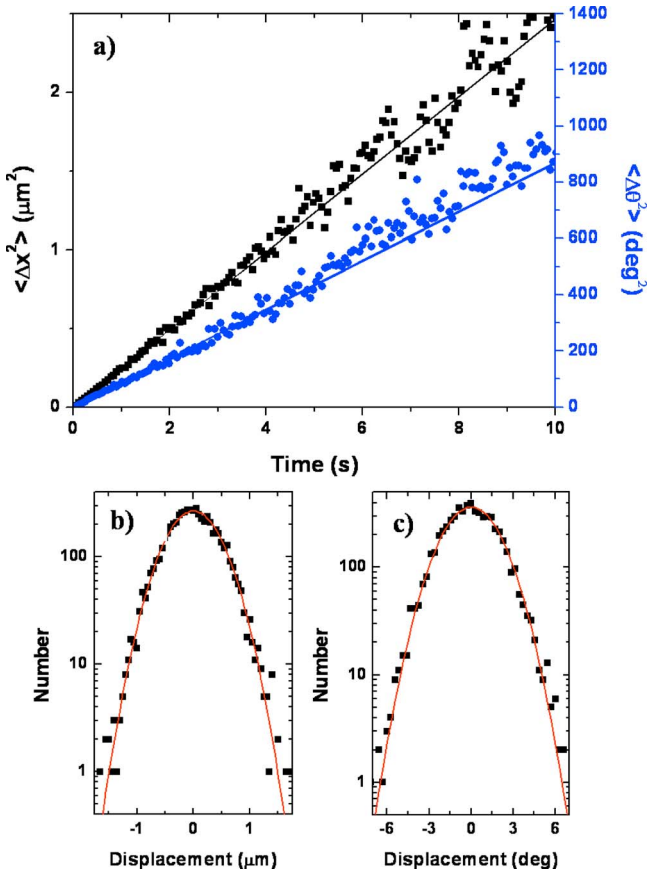

FIG. 4. (Color online) Examples of raw dynamic data. (a) Mean-squared translational displacement (squares) and rotational displacement (circles) plotted against time for a linear cluster of four particles [Fig. 1(d)]. Lines through the data are linear regressions. (b) Distribution of step size of translational displacement (known as the van Hove distribution), plotted here regarding the time interval of 60 ms. (c) Distribution of step size of rotational displacement, plotted regarding the time interval of 60 ms. Lines through the data in (b) and (c) are fits to the Gaussian distribution expected for Fickian motion.

For perspective, it has long been known for dilute spheres in the bulk that the translational diffusion constant is given by the Stokes–Einstein relation,

$$D_{t0} = \frac{k_B T}{6\pi\eta r}, \tag{5}$$

and the rotational diffusion constant is given by the Debye–Stokes–Einstein relation,

$$D_{r0} = \frac{k_B T}{8\pi\eta r^3}, \tag{6}$$

where T is the temperature, η is the viscosity of the medium, and r is the radius of the sphere.

TABLE I. Tabulated translational and rotational diffusion coefficients (D_t and D_r, respectively) for the shapes depicted in Figs. 1 and 6(a). The uncertainty ("Unc") column is the standard deviation from fits of the mean-squared displacement to time elapsed. For each shape, the inertial radius of gyration (R_g) in units of micrometers was determined. There was a strong inverse correlation (0.97) between the radius of gyration and the rotational diffusion coefficient. However, the radius of gyration fails to capture the full picture, since at low Reynolds numbers, inertia is not the proper representation of hydrodynamic interaction. The aspect ratio, here chosen to be the maximum ratio of one axis to the axis orthogonal to it within the plane, was also determined, but was not found to strongly correlate with diffusion constants.

No. of particles	D_t (μm^2/s)	(Unc)	D_r (deg^2/s)	(Unc)	D_r/D_t	(Unc)	R_g	Aspect ratio	Shape	Shown at
1	0.165		1099		6644		0.5	1.0	Point	
2	0.111	0.013	251	38	2300	610	0.9	2.0	Linear	a
3	0.082	0.004	99	3	1200	100	1.4	3.0	Linear	b
3	0.085	0.008	189	21	2200	400	1.0	1.1	Triangle	c
4	0.062	0.001	43	2	710	50	1.8	4.0	Linear	d
4	0.070	0.004	121	14	1700	300	1.2	1.4	Diamond	e
4	0.072	0.003	118	10	1600	200	1.2	1.0	Square	f
4	0.067	0.004	83	9	1200	200	1.4	1.6		g
4	0.072	0.001	87	2	1200	100	1.4	1.4	T-shape	h
5	0.055	0.004	71	6	1300	200	1.4	1.6	Trapezoid	i
5	0.064	0.001	62	3	970	50	1.6	1.9		j
5	0.053	0.003	51	2	960	90	1.7	1.3		k
5	0.062	0.009	79	4	1300	300	1.5	1.4	Bowtie	l
6	0.057	0.001	45	2	800	50	1.7	1.8		m
6	0.052	0.001	50	3	960	90	1.6	1.9	Parallelogram	n
6	0.050	0.004	61	7	1200	200	1.5	1.1		o
6	0.050	0.002	44	3	870	90	1.8	2.1		p
6	0.054	0.004	45	3	840	120	1.5	1.1	Triangle	q
7	0.045	0.001	59	3	1300	100	1.5	1.1	Hexagon	r
8	0.039	0.001	29	2	740	80	2.0	2.4	Parallelogram	s
9	0.036	0.001	31	3	860	90	1.9	1.5	Diamond	t

B. Influence of the nearby wall

The presence of a nearby solid wall retards translational diffusion. For a sphere, it has long been known that diffusivity parallel to the wall (D_t) relative to unbounded bulk diffusion (D_{t0}) is given by

$$\frac{D_t}{D_{t0}} = 1 - \frac{9}{16}\frac{r}{z} + \frac{1}{8}\left(\frac{r}{z}\right)^3 - \frac{45}{256}\left(\frac{r}{z}\right)^4 - \frac{1}{16}\left(\frac{r}{z}\right)^5, \tag{7}$$

where r is the radius of the sphere and z is the separation of the center of the sphere from the wall.[11,12] Thus, for a sphere, the translational diffusion coefficient diminishes by at most 2/3.

C. Clusters

As a qualitative guide of what to expect in the way of translational diffusion, the component particles can be considered as independent. Their translational diffusivity is then reduced as if for a single sphere but their separation from the wall follows the Boltzmann distribution expected from gravity and hence depends on mass of the entire cluster. The expected reduction in translational diffusivity then depends on the mass of the cluster. For particles of the size studied in this paper, it falls from 55% of the bulk value, for a single sphere, to 36% of the bulk value, for clusters of nine particles. For each of the particle sizes that were studied, Fig. 2 shows this computation.

When considering rotation, wall effects are inherently weaker. For spheres, the lowest-order solution based on solving the Langevin equation can be shown to be

$$\frac{D_r}{D_{r0}} = 1 - \frac{1}{8}\left(\frac{r}{z}\right)^3, \tag{8}$$

where r is the radius of the sphere and z is the separation of the center of the sphere from the wall.[13] For the range of mean wall separations shown in Fig. 1, this leads to expecting rotation to be slowed from 94% to 89% of the bulk value. Going beyond the spherical approximation, it is not clear what to expect, as the axis of rotation for a sphere lies through the sphere's closest point of approach to the wall, but the same does not hold for a cluster. Fortunately, the influence on rotation is weaker to begin with, and thus given the large changes we observed in D_r, unlikely to be the dominant factor. At the same time, we cannot discount the possibility that some of the trends reported below might include contributions from the presence of the nearby wall.

D. Clusters of different size and shape

For the clusters depicted in Fig. 1, their translational and rotational diffusion coefficients are summarized in Table I.

Seeking to generalize, we offer some qualitative observations. First, Fig. 5 shows the addition, one sphere at a time, of spheres to a central sphere. Eventually this forms a filled hexagon, six spheres in a hexagon around the original sphere; the intermediate stages of filling are also shown. To add a second sphere causes the rotational diffusion to drop quite dramatically to less than a quarter of its original value, while the drop in translational diffusion is much less

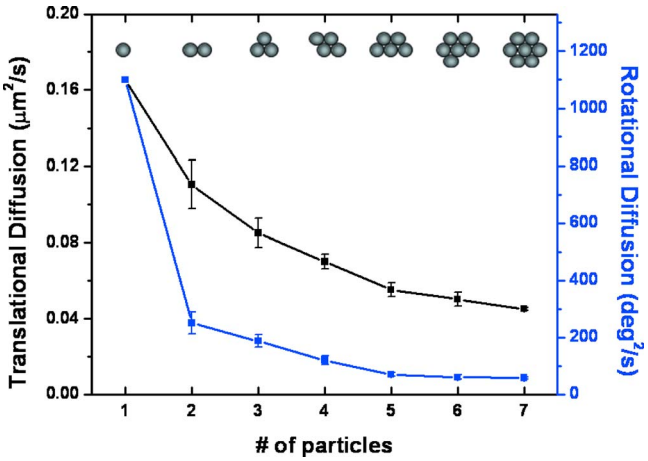

FIG. 5. (Color online) Translational diffusion coefficient D_t (squares) and rotational diffusion coefficient D_r (circles) are shown for a series of clusters in which spheres are sequentially added to a central sphere until six have been added to form a hexagon. One observes that whereas D_t decreases smoothly and nearly exponentially, D_r displays three distinct zones: Precipitous drop upon adding the first sphere, steady decline as the next three spheres are added, then plateau for the final two spheres. As a result, changes in the effective hydrodynamic radius for translation and rotation are significantly decoupled.

pronounced, remaining at 2/3 of its original value. To add the next three particles to the cluster continues to widen the ratio between rotational and translational diffusions, yet the rotational diffusion coefficient ceases to drop so precipitously, decreasing by a slightly lesser fraction in these three steps combined than in the first step. Clearly, translation and rotation diffusion coefficients do not change in step with one another.

Most interesting of all is the contrasting influence, on rotation and translation, of adding the final two particles. The rotational diffusion coefficient remains the same within experimental uncertainty, indicating nearly the same hydrodynamic radius for rotation, probably because the average distance of the outer spheres from the center of mass of the cluster is nearly unchanged. But translational mobility decreases, each accreted sphere increasing the minimum cross section of the cluster. This explains why, upon adding the final particle, the ratio D_r/D_t, which, previously decreased, now increases: the higher effective hydrodynamic radius for translation is no longer accompanied by higher hydrodynamic radius for rotation. Our observations thus include cases where the effective hydrodynamic radius changes more rapidly for translation than rotation, the converse, and also the cases where the effective hydrodynamic radius for translation changes significantly, while that of rotation is effectively constant.

Figure 6(a) summarizes the consequence of changing independently the size of the cluster and its symmetry. Note the mirror symmetry of this table across the diagonal axis from the upper left to the lower right. Along this diagonal, the number of spheres in the cluster increases; the shapes are parallelograms whose aspect ratio differs. Moving from this diagonal midline signifies primarily that the number of spheres is the same but the shape is increasingly extended. Representative slices along each axis are summarized in

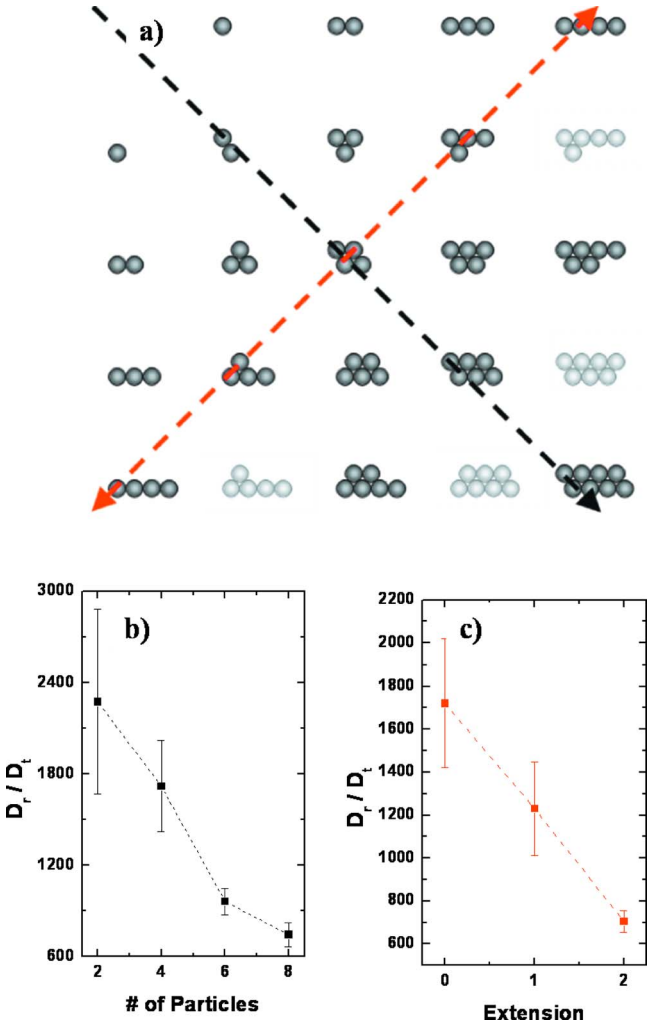

FIG. 6. (Color online) Data presented in a fashion to display semi-independently the consequences of changing the number of spheres in the cluster and its shape. (a): Along the downward-sloping diagonal, the cluster grows in size with minimal change in shape, as denoted by a line. The image is symmetric across this axis. Leaving this diagonal, the number of spheres in the cluster is constant but the conformation is increasingly extended, as denoted by the upward-sloping line. Data for all of these cases, except for the semitransparent ones, are tabulated in Table I. (b): Following a path parallel to the diagonal in (a), the ratio D_r/D_t decreases. (c): Following a path perpendicular to the diagonal in (a), the ratio D_r/D_t decreases. (b) and (c) are presented as to summarize qualitative trends evident from close inspection of situations tabulated in Table I.

Figs. 6(b) and 6(c). Seeking to generalize, we observe that upon increasing the cluster size while maintaining a relatively consistent shape, both D_r and D_t decrease smoothly, as does their ratio D_r/D_t. The same qualitative trend holds when maintaining the same number of particles in the cluster and extending the cluster geometry.

The significance of this work, beyond the quantitative data summarized in Table I, is to validate a new experimental platform in which to explore the connections between rotational and translational diffusions at the single-particle level for geometrical shapes not described by the Stokes–Einstein–Debye equations for spherical particles. In future work, it will be interesting to extend this approach to crowded situations where hydrodynamic interactions between clusters come into play.

ACKNOWLEDGMENTS

S.A. acknowledges the NSF for financial support in the form of a Graduate Research Fellowship. This work was supported by the National Science Foundation Grant No. NSF-DMR-06-05947.

[1] J. D. Joannopoulos, P. R. Villeneuve, and S. H. Fan, Nature (London) **386**, 143 (1997).
[2] J. H. Holtz and S. A. Asher, Nature (London) **389**, 829 (1997).
[3] M. E. Leunissen, C. G. Christova, A. P. Hynninen, C. P. Royall, A. I. Campbell, A. Imhof, M. Dijkstra, R. van Roij, and A. van Blaaderen, Nature (London) **437**, 235 (2005).
[4] E. R. Weeks, J. C. Crocker, A. C. Levitt, A. Schofield, and D. A. Weitz, Science **287**, 627 (2000); W. K. Kegel and A. van Blaaderen, *ibid.* **287**, 290 (2000).
[5] A. M. Alsayed, M. F. Islam, J. Zhang, P. J. Collings, and A. G. Yodh, Science **309**, 1207 (2005); P. Schall, I. Cohen, D. A. Weitz, and F. Spaepen, Nature (London) **440**, 319 (2006).
[6] Y. Han, A. M. Alsayed, M. Nobili, J. Zhang, T. C. Lubensky, and A. G. Yodh, Science **314**, 626 (2006).
[7] D. Mukhija and M. J. Solomon, J. Colloid Interface Sci. **314**, 98 (2007); R. Cush, D. Dorman, and P. S. Russo, Macromolecules **37**, 9577 (2004).
[8] L. Hong, S. M. Anthony, and S. Granick, Langmuir **22**, 7128 (2006).
[9] R. D. Deegan, O. Bakajin, T. F. Dupont, G. Huber, S. R. Nagel, and T. A. Witten, Nature (London) **389**, 827 (1997).
[10] S. Anthony, L. F. Zhang, and S. Granick, Langmuir **22**, 5266 (2006); J. C. Crocker and D. G. Grier, J. Colloid Interface Sci. **179**, 298 (1996).
[11] The factor of 1/8 in Eq. (7) corrects a typo of S. M. Anthony, L. Hong, M. Kim, and S. Granick, Langmuir **22**(24), 9812 (2006), an earlier publication from this laboratory.
[12] L. P. Faucheux and A. J. Libchaber, Phys. Rev. E **49**, 5158 (1994).
[13] J. Happel and H. Brenner, *Low Reynolds Number Hydrodynamics with Special Applications to Particulate Media*, 1st ed. (Prentice Hall, Englewood Cliffs, 1965).